EFFECTS OF MUD COMPRESSIBILITY ON WELLBORE CLOSURE AND ANNULAR PRESSURE BASED ON FEM WITH THE INCORPORATION OF FLUID ELEMENTS

Daniel Duque Estrada Fernandes de Melo

Juan David V. Uribe, Sergio A. B. da Fontoura and Nelson Inoue

danielduquemelo@puc-rio.br

juandavid@ puc-rio.br; fontoura@ puc-rio.br; inoue@ puc-rio.br

PUC-Rio

Rua Marques de São Vicente 255, 22451-900, Rio de Janeiro, RJ, Brazil

Jorel L. R. Anjos

jorel.anjos@petrobras.com.br

Petróleo Brasileiro S.A.

Av. Horácio Macedo 950, 21941-915, Ilha do Fundão, Rio de Janeiro, RJ, Brazil

Abstract. *In recent years, a significant number of sub-salt reservoirs have been discovered. As a result, wells are required to be drilled through salt layers, which can be thicker than 2000 meter. Salt time-dependent behavior can present a high/slow mobility rate, which may lead to major drilling problems. To predict wellbore effective diameter, Finite Element Analysis (FEA) are commonly used. Generally, FEA estimates the radial displacement based on constant mud pressure described as a distributed load on wellbore surface. Although it is a good approximation for the drilling phase, it can underestimate displacements in confined annular after casing set up. With the incorporation of fluid elements, the present work shows the impact of mud compressibility on the wellbore radial displacement. Based on parametric FEA for different mud compressibility, a significant displacement reduction was observed with the increase of fluid bulk modulus. For nearly incompressible fluids in trapped annulus, radial closure is significantly smaller. Furthermore, it is shown that the incorporation of fluid elements lead to displacement errors on order of 60% on deeper depths. From the results of two salt layers (1000 meters and 2000 meters), minimum casing internal pressure was calculated based on mud weight and annular pressure build-up due to salt creep.*

Keywords: *Salt creep, annular pressure build-up, and finite element method*

1 INTRODUCTION

Due to salt low porosity and low permeability, these formations represent a significant percentage of reservoirs' sealing rock. In order to reach these hydrocarbon accumulations, many wells must cross long layers of salt, which increase uncertainties about its integrity. For deep wells, a proper casing design has to be carefully analyzed to guarantee a safe operation until well abandonment.

When crossing long salt sections, intermediary casing has a major role, as it must protect production casing from salt-related problems. To assure well integrity, a series of studies have to be conducted to determine whether the casing configuration will withstand different types of loads over time.

After casing settlement, the drilling mud in outer annulus becomes confined between casing hanger and top of cement. As salt creeps, wellbore closure pressurizes trapped fluid, increasing intermediary casing load. The amount of pressure build-up will be directly related to fluid compliance.

This paper focuses on a finite element method (FEM) analysis of the effects of fluid compliance on the wellbore closure and casing integrity. The model consists of a 17 1/2" well with a 13 3/8" intermediary casing (72 lb/ft, P110 steel). Based on axisymmetric models, wellbore displacement and casing minimum internal pressure were analysed for a 1000 meters and a 2000 meters homogeneous salt sections.

2 MATERIALS BEHAVIOR

Salt time-dependent behavior lead to slow deformation over time when submitted to any differential stresses. Strain rates are also dependent of Salt impurities, temperature and mineralogical composition (Fjaer et al., 2008 and Liu Wei et al., 2013). The most mobiles salts are carnalite and taquihydrite while halite has a slower mobility rate.

There are different constitutive laws that represent viscous-elastic deformation of rocks. In this paper, a double mechanism creep law is adopted according to Eq. (1). From experiments reported in the literature at reference temperature of 86°C and different differential stresses, steady-state creep rates are showed in Figure 1 (Poiate et al., 2006). Interestingly, as it can be seen in the figure, taquihydrite and halite have a higher strain rate for differential stresses over 7 MPa and 9.9 MPa, respectively.

$$\dot{\varepsilon} = \varepsilon_0 \left(\frac{\tilde{q}}{\sigma_0} \right)^n \exp\left(\frac{Q}{R\theta_0} - \frac{Q}{R\theta} \right) \tag{1}$$

Where ε_0 is the experiment reference strain rate, $\tilde{q}$ is Von Mises differential stress, σ_0 is experiment reference differential stress, n is the stress-strain rate power coefficient, Q = 12 Kcal/mol, R =1.9858x10^{-3} kcal/(mol*K), θ_0 is experiment reference temperature, θ is the material temperature.

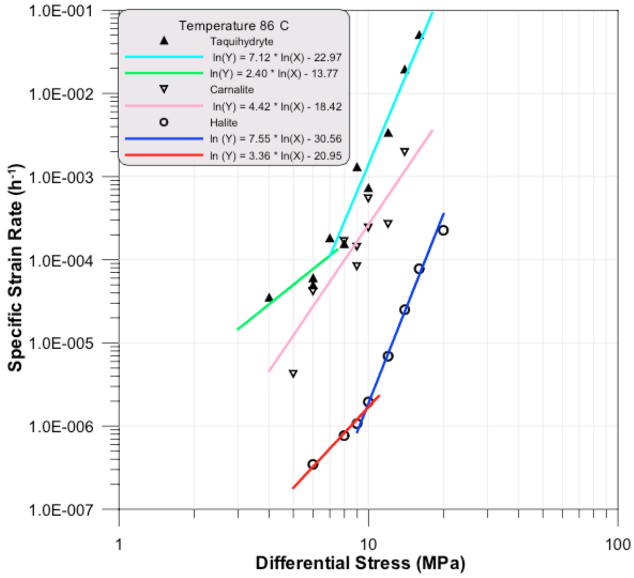

Figure 1. Strain rate for different differential stresses for salt rocks (Poiate et al., 2006).

Regarding pipe collapse, American Petroleum Institute (2008) indicates the occurrence of four collapse types depending on diameter to thickness ratio (slenderness ratio): yield strength collapse, plastic collapse, transition collapse and elastic collapse (Figure 2).

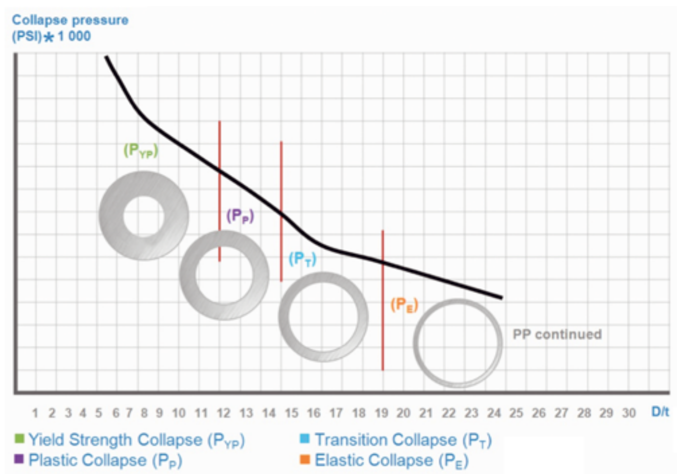

Figure 2. Type of collapse as function of slenderness ratio according to API 5C3.

There are a few analytical equations to determine critical collapse pressure (Timoshenko and Gere, 1961; Clinedinst, 1940; Klever and Tamano, 2004). For oilfield casing and tubing, API 5C3 indicate that Klever-Tamano equation have the best fit for a wide range of pipes. With the accountability of material plasticity and tube imperfections, ultimate collapse pressure can be calculated as per Eq. (2).

$$P_c^{KT} = \frac{\left(P_e^{KT} + P_y^{KT}\right) - \sqrt{\left(P_e^{KT} - P_y^{KT}\right)^2 + 4H_t P_y^{KT} P_e^{KT}}}{2\left(1 - H_t\right)} \qquad \text{(2-a)}$$

$$P_e^{KT} = k_{eu} 2E_e \left(\frac{D}{t}\right)^{-1} \left(\frac{D}{t} - 1\right)^{-2} \tag{2-b}$$

$$P_y^{KT} = k_{yu} 2\sigma_y \left(\frac{D}{t}\right)^{-1} \left[1 + \frac{1}{2}\left(\frac{D}{t}\right)^{-1}\right] \tag{2-c}$$

$$H_t = 0.127OV - 0.0039Ecc - 0.44\left(\frac{\sigma_{rs}}{\sigma_y}\right) + h_n \tag{2-d}$$

Where D is casing outer diameter, t is tube wall thickness, σ_y is steel yield stress, k_{eu}=1.081, k_{yu}=0.9911, OV is ovality, Ecc is eccentricity, σ_{rs} is steel residual stress and h_n is steel stress-strain curve shape factor.

Based on the creep constitutive law, pressurization of annulus can be accounted as function of fluid compliance and annulus volume change. Since fluid comprises the annular section from top of cement to wellhead, the bulk modulus on mobile region on salt region (volume V_C) must be corrected with respect of no-creep sections volume (V_{NC}), as presented in Eq. (3).

$$K = \left(-V_C \frac{\partial P}{\partial V}\right)\left(\frac{V_C}{V_{NC} + V_C}\right) \tag{3}$$

3 ANULAR PRESSURIZATION

For the annular pressurization, a 17.5 in well was considered. The wellbore closes over a 13 3/8 in, 72 lb/ft, P110 casing, which collapses under 26.4 MPa based on Klever-Tamano equations (Equation (2)). The analysis of fluid effects on wellbore considered two Halite sections and four different fluids. The model consists on axisymmetric analysis of the complete Salt section over 10 years. For the simulation, 4-nodes quadrilateral elements were used, with vertical length of 1 meter each. Regarding salt creep, a FORTRAN subroutine computes creep strain rates based on Eq. (1).

The characteristics of both salt sections are in Table 1. For both cases, specific weights were fixed at 1000 kg/m³ for seawater, 2293.5 kg/m³ for sediments above salt, and 2053 kg/m³ for halite. With the seabed temperature at 4°C, it was assumed a geothermal gradient of 0.048°C/m and 0.0073°C/m for sediments above salt and halite, respectively.

The annular fluid had a 10.5 ppg (1258.2 Kg/m³) density. The initial mud pressure was simulated with triangular distributed load on wellbore face. In addition, it was incorporated hydrostatic fluid elements to account for fluid compliance. Thus, four parametric simulations were carried to evaluate effects of fluid compressibility, as per Table 2. The first simulation did not consider fluid compressibility (annular open to environment), which is the most commonly used, while the others considered fluids with 1200 MPa, 1500 MPa and 1800 MPa bulk modulus, respectively.

Table 1. Salt and water depth for the two models simulated

	Section 1 (1000 m)	Section 2 (2000 m)
Water Depth	2000 m	2000 m
Salt top	3500 m	3000 m
Salt bottom	4500 m	5000 m

Table 2. Fluid scenarios for parametric study

	Case 1	Case 2	Case 3	Case 4
Fluid Bulk Modulus (K)	0 MPa	1200 MPa	1500 MPa	1800 MPa

3.1 1000 metres halite section

For the 1000 meters salt section, overburden stresses start with 53.67 MPa at Salt top and increase linearly to 73.5 MPa, while temperature increase from 76°C to 83.3°C. Based on fluid properties, mud pressure on wellbore linearly increase from 43.2 MPa and 55.5 MPa at Salt top and bottom, respectively.

Figure 3 present the results of effective wellbore and annular pressure build-up for the four different fluids simulated. It can be seen that the incorporation of fluid compressibility significantly decreases wellbore displacement (Figure 3a). This decrease occurs mainly due to annular pressure increase, which are about 10 to 10.5 MPa for all three fluids, as shown in Figure 3b. The difference among the three fluids confined (with non-zero bulk modulus) is less significant though.

Figure 4 shows the displacement error percentage between confined fluids models (cases 2,3 and 4) and non-confined fluid model (case 1). As it can be seen, the percentage of error can be as high as 23%, indicating that compressibility must be considered when annular is confined.

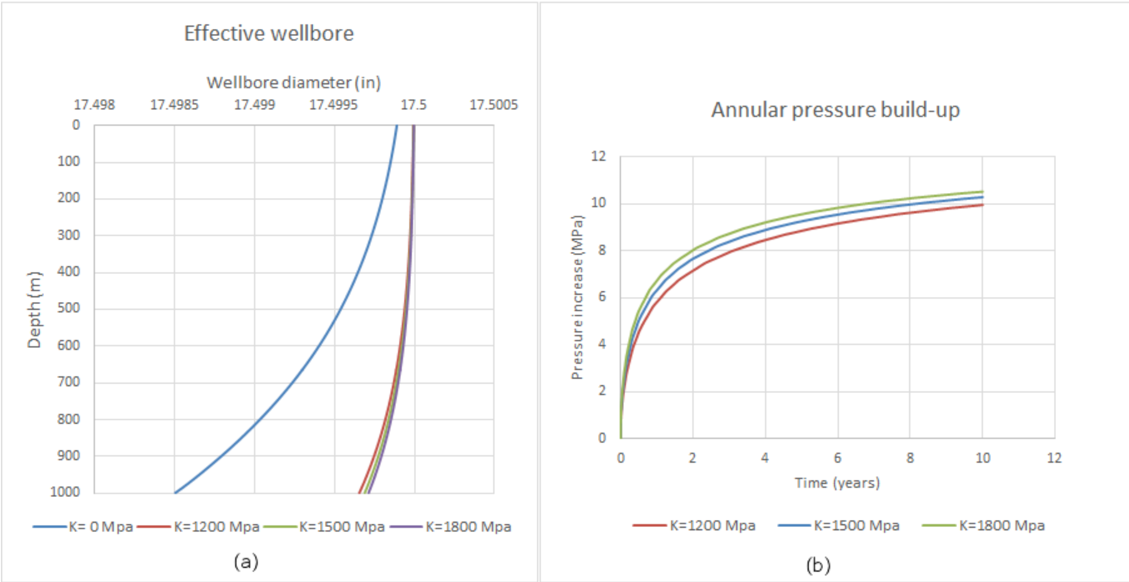

Figure 3. Effective wellbore and annular pressure increase for the 1000 meter salt section.

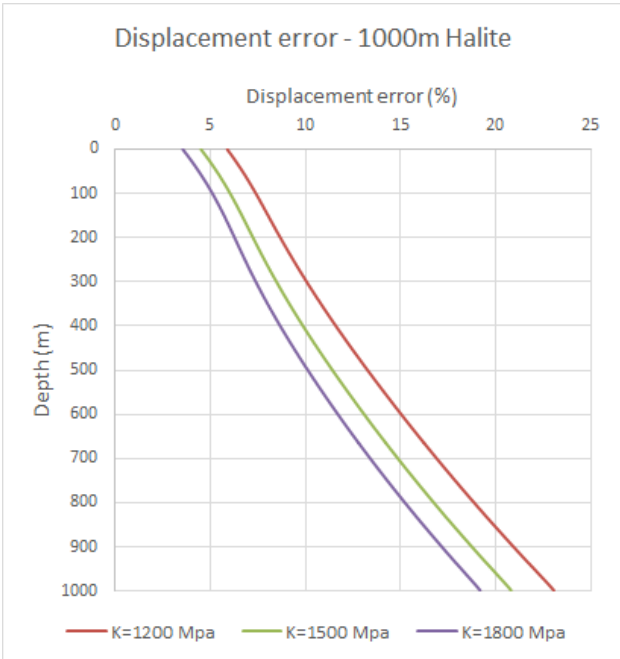

Figure 4. Displacement error between confined and open annulus for the 1000m Halite section

3.2 2000 meters Halite Section

For the 2000 meters Salt section, its top is submitted to 42.1 MPa overburden stresses, 70°C temperature and 37 MPa mud pressure. At its bottom, loads are 82.0 MPa stress, 90°C temperature and 61.7 MPa mud pressure. Figure 5 show the results of wellbore closure (a) and annular pressure increase (b) for the model. For a 2000 meters salt section, effective diameter at bottom is significantly smaller than at the top. When considering fluid compressibility, Figure 5b shows that for all three fluids annular pressure increase about 6.6 MPa.

For the 2000 meter section, a different trend in displacement error percentage can be seen (Figure 6) between confined fluids models (cases 2,3 and 4) and non-confined fluid model (case 1). At the top of Salt, confined fluid models have lower displacements, while at bottom these displacements are up to 60% higher when compared to open annulus model. This indicates that due to high displacements of deeper formations (high stress magnitudes) fluid is dislocated to shallower region, where fluid pressure overcome overburden stress.

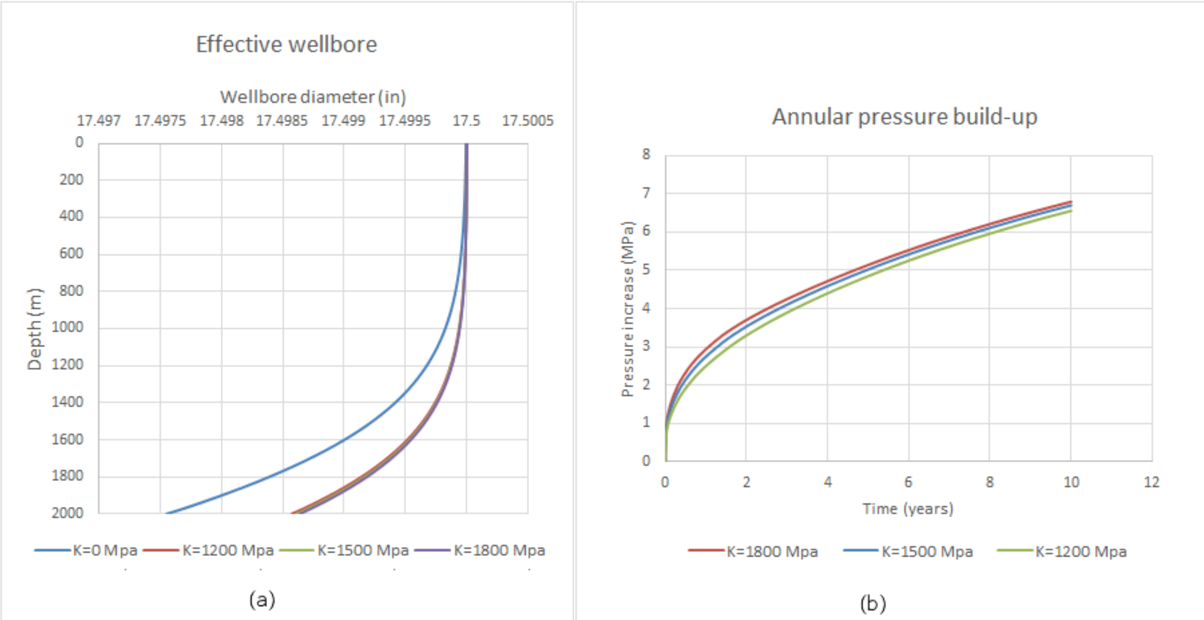

Figure 5. Effective wellbore and annular pressure increase for the 1000 meter Salt section.

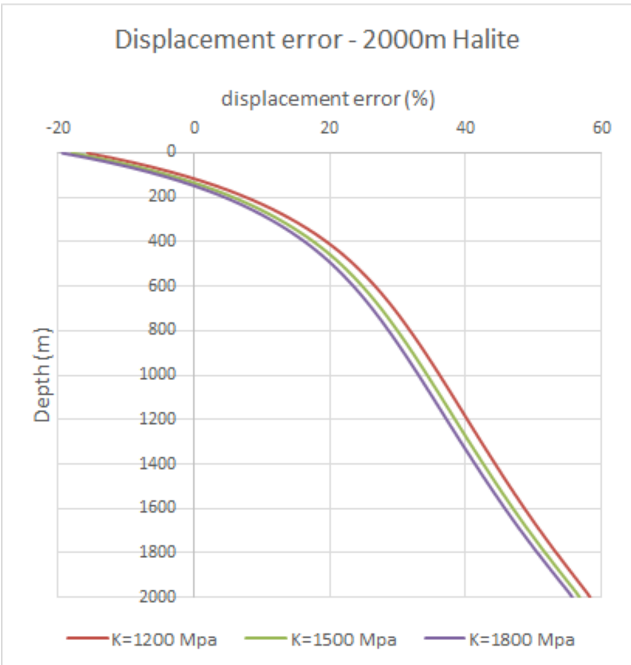

Figure 6. Displacement error between confined and open annulus for the 2000m Halite section

3.3 Casing collapse limit

Considering the worst-case scenario for casing collapse, which is 1800 MPa Bulk modulus, Figure 7 shows annular pressure per depth for both Salt sections. For the 13 3/8 in casing, limiting internal pressure can then be calculated based on the difference between external pressure and ultimate collapse pressure. To guarantee casing integrity over 10 years through the 1000 meters Halite formation, internal pressure must be higher than 34 MPa. For the 2000 meters section, internal pressure cannot lower to less than 42.5 MPa. Therefore, these limiting pressures must be taken into account before production phase, where operations such as gas lift can jeopardize well integrity.

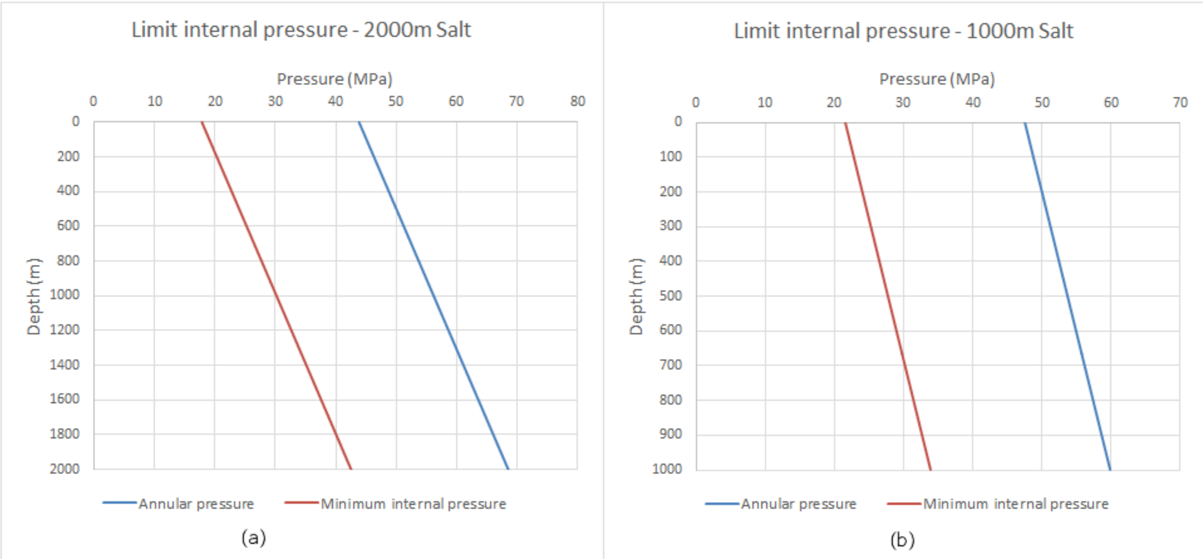

Figure 7. Effective wellbore and annular pressure increase for the 1000 meter Salt section.

4 CONCLUSIONS

From the axisymmetric model, two Halite sections where simulated based on different fluid properties. From the results obtained, it is clear that the effect of annular confinement and fluid compressibility have a major impact in wellbore displacement and pressure on casing. When comparing an open-to-surface annulus (K=0 MPa) to confined annulus (K≠0 MPa), wellbore displacements are miscalculated up to 60%.

For long salt sections, greater stress magnitude differences from formation top to its bottom can lead to fluid dislocation upwards. Thus, annular pressure increase may lead to horizontal stresses lower than mud pressure in shallower regions, which lead to wellbore opening.

From the two analyses, limiting casing internal pressure could be estimated to avoid its collapse. For the 1000 meters Halite section, well internal pressure must not lower less than 34 MPa, while this threshold is 42.5 MPa for the 2000 meters formation.

REFERENCES

AMERICAN PETROLEUM INSTITUTE. 2008. API 5C3: Technical Report on Equations and Calculations for Casing, Tubing, and Line Pipe Used as Casing or Tubing; and Performance Properties Tables for Casing and Tubing. Washington, 2008.

Timoshenko, S.; J.M. Gere. 1961. Theory of elastic stability., 2nd. ed., New York : MacGraw-Hill Book Company , 1961

Clinedinst, W.O. 1940. A Rational Expression for the Critical Collapsing Pressure of Pipe Under External Pressure. API Chicago meeting 1939, pub. API, 1940

Klever, F.J., T. Tamano. 2004. A New OCTG Strength Equation for Collapse Under Combined Loads, SPE-90904-MS, SPE Annual Technical Conference and Exhibition, 26-29 September, Houston, Texas, 2004

Fjaer, E., R.M. Holt, P. Horsrud, A.M. Raaen, R. Risnes. Petroleum Related Rock Mechanics. Elsevier Science Publishers B.V, 2008.

Liu Wei, L. Yinping, Y. Chunhe, H. Shuai, W. Bingwu. 2013 Analysis of physical and mechanical properties of impure salt rock. ARMA 13-336;

Poiate, E.J., A.M. Costa, & J.L. Falcão. 2006. *Well design for drilling thick evaporite layers in Santos basin – Brazil. SPE paper 99161.* This paper was selected for presentation in the IADC/SPE Drilling Conference held in Miami, Florida, U.S.A., 21–23 February 2006.